Levitated electrons

V. S. Edel'man

Institute of Physical Problems, Academy of Sciences of the USSR
Usp. Fiz. Nauk **130**, 675–706 (April 1980)

Experimental and theoretical work is reviewed on the two-dimensional system of electrons suspended above the surfaces of certain cryogenic dielectrics (liquid ^{3}He and ^{4}He and liquid and solid hydrogen) by the image force and an external electrostatic field. The stability of the system is studied. The electron properties determined by the interactions of the electrons with each other, with vapor atoms, and with thermal vibrations of the liquid surface are studied. A study of nonlinear effects is reported.

PACS numbers: 67.90. + z, 41.70. + t

CONTENTS

1. INTRODUCTION

The electrification of dielectrics has been recognized for thousands of years, and the study of this effect was essentially the starting point for the science of electricity. It was only very recently, however, that Cole and Cohen[1] and, independently, Shikin[2] pointed out that the electrification is very unusual if the permittivity ε is approximately one (liquid ^{4}He, for example, with $\varepsilon_4 = 1.0572$; Ref. 3) and if the electron affinity is negative. To illustrate the effect of the difference $\varepsilon - 1$ being small we examine the behavior of a free electron above a dielectric surface.

The electron is of course attracted to the surface by an electrostatic image force, which is described by the potential[4]

$$\varphi(z) = -\frac{e^2(\varepsilon-1)}{4(\varepsilon+1)z} = -\frac{Qe^2}{z}, \qquad (1)$$

where z is the coordinate normal to the surface. The electron should thus approach the surface and remain somewhere in its vicinity, not actually penetrating into the dielectric since the energy of the extra electron inside the material would be greater than outside (Fig. 1; for ^{4}He, the height of the corresponding potential barrier is[1] 1 eV). Stationary states form in the resulting one-dimensional well, and their energy can be estimated easily from the virial theorem,[5] which in this case leads to the equation $2p^2/2m = Qe^2/z$, and from the uncertainty relation $p \cdot z \approx \hbar$. From these equations we find the binding energy to be

$$E_b = -\frac{p^2}{2m} = -\frac{mQ^2e^4}{2\hbar^2}. \qquad (2)$$

Substituting ε_4 into (2), we find $E_b = 1.05 \cdot 10^{-15}$ erg and a typical distance $z = 76$ Å. We thus see that when the difference $\varepsilon - 1$ is small the condition $z \gg a$ will hold, where a is the spacing of the atoms. In contrast, at the values $\varepsilon - 1 \gtrsim 1$ typical of most dielectrics we would have $z \approx a$. In the case of a small difference $\varepsilon - 1$, the electrons remain held far from the surface, so that they are evidently free to move parallel to it. In the case of a large difference, the electrons are instead bound to specific atoms of the material or to crystal defects, and the resulting picture is one of ordinary electrification.

In summary, the electrons trapped above a dielectric for which the difference $\varepsilon - 1$ is small form a two-dimensional conducting system: a new physical object, which presents a problem to be investigated. The study should be directed toward answering the following basic questions:

1) With which materials can electrons form bound states exhibiting a two-dimensional conductivity?

2) What is the stability of the resulting system?

3) What is the phase state?

4) What are the properties of the bound electrons, and how are these properties affected by the interaction

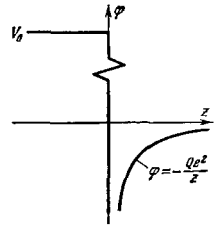

FIG. 1. Potential diagram of the forces acting on an electron near a helium surface.

 0038-5670/80/040227-18$01.10

with the surrounding medium and with external electric and magnetic fields?

These questions have been covered to varying degrees in previous reviews.[6-9] The recent appearance of new work now permits a more complete description of the properties of the two-dimensional conducting system of electrons trapped above a dielectric.

2. ELECTRON SPECTRUM ABOVE LIQUID HELIUM

It is clear from the estimates above that for an electron above liquid helium the potential in (1) gives a good description of the interaction with the liquid along the normal to the surface, because the electron is quite remote from the surface. Since the motion parallel to the surface is free motion (if we ignore the interaction with surface vibrations), the Schrödinger equation splits into two parts. One part has the solution

$$\Phi(x, y) = Ae^{i\mathbf{pr}} = Ae^{i\mathbf{vr}/m}, \tag{3}$$

where **r** is the position vector in the plane of the surface, and m is the mass of a free electron. For motion along the z axis at $z>0$ we have[6,7]

$$-\frac{\hbar^2}{2m}\frac{d^2\Phi_l}{dz^2}+\varphi(z)\Phi_l=E_l\Phi_l \tag{4}$$

and if the barrier is assumed to be infinite at the origin of coordinates we have $\Phi_l(z)=0$ at $z<0$. Equation (4) can be solved by analogy with the well-known Schrödinger equation for the hydrogen atom. The energy eigenvalues E_l differ from those for the hydrogen atom only by a factor Q^2; they are

$$E_l=-\frac{Q^2me^4}{2\hbar^2l^2}. \tag{5}$$

It can be seen from (5) that E_1 agrees with the estimate in (2). The normalized wave functions for the first three states are

$$\begin{aligned}\Phi_1(z)&=2\gamma^{3/2}ze^{-\gamma z},\\ \Phi_2(z)&=\frac{\gamma^{3/2}}{\sqrt{2}}ze^{-\gamma z/2}\left(1-\frac{\gamma z}{2}\right),\\ \Phi_3(z)&=\frac{2}{3\sqrt{3}}\gamma^{3/2}ze^{-\gamma z/3}\left(1-\frac{2\gamma z}{3}+\frac{2\gamma^2z^2}{27}\right),\end{aligned} \tag{6}$$

with an effective Bohr radius

$$\frac{1}{\gamma}=\frac{\hbar^2}{mQe^2}. \tag{7}$$

Substituting $\varepsilon_4=1.0572$ into Q, we find $1/\gamma=7.6\cdot10^{-7}$ cm, and we find the average distance between the electron and the helium surface in the ground state to be $\langle z\rangle_1=6/4\gamma=114$ Å. In this approximation, we find $\langle z\rangle_2=456$ Å, $\langle z\rangle_3=1026$ Å.

The solution in (5) gives a good description of the actual spectrum. For the frequencies corresponding to transitions from the $l=1$ ground state to the $l=2$ and 3 excited states, for example, we find $F_{12}=119.7$ GHz and $F_{13}=141.8$ GHz from (5), while direct measurements by Grimes *et al.*[10] yield 125.9 ± 0.2 and 148.6 ± 0.3 GHz. If we take into account the finite barrier height $V_0=1$ eV at the boundary[1,11] and replace the potential in (1) by

$$\varphi(z)=\frac{Qe^2}{z+\beta}, \tag{8}$$

where we have eliminated the divergence at $z=0$, we

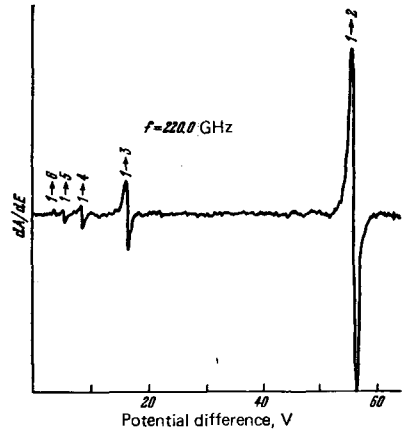

FIG. 2. Derivative of the absorption of the 220-GHz signal by electrons as a function of the potential difference applied to the capacitor plates.[10] The helium level is at the center of the capacitor, with a gap of 3.18 mm. The helium temperature is 1.2 K.

can correct the calculation and reach agreement with experiment[10] by adopting the reasonable value $\beta_4=1.04$ Å.

The electrons will evidently remain above the liquid if a not too strong static electric field $E_\perp$ is applied along the normal to the surface in the direction such that it pushes the electrons toward the surface. This field will change the energy eigenvalues E_l, because there will be a change $eE_\perp z$ in the potential energy. Since the function $\Phi_l(z)$ is not symmetric with respect to z, the expectation values $\langle z\rangle_l=\langle\Phi_l z\Phi_l\rangle$ are not zero, and even in first-order perturbation theory we find corrections to E_l; they are

$$\Delta E_l=eE_\perp\langle z\rangle_l. \tag{9}$$

The fact that the energy spectrum can be changed by an external field is of much help experimentally. In their experiments, Grimes *et al.*[10] found the transition frequencies by studying the absorption of a microwave signal at a fixed frequency while varying $E_\perp$ monotonically. The measurement sensitivity was improved by imposing a small-amplitude 100-kHz alternating field on the slowly varying field $E_\perp$. The quantity detected was thus proportional to the derivative of the absorption signal (Fig. 2). A change in the transition frequencies which was linear in the field was observed only at low values of $E_\perp$ (Fig. 3). The reason for this re-

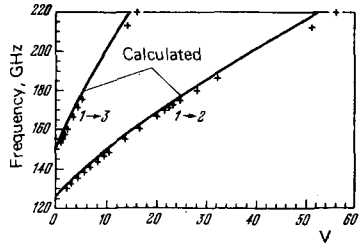

FIG. 3. Dependence on the retarding potential of the frequencies of the $1\rightarrow2$ and $1\rightarrow3$ transitions in the spectrum of electrons trapped above liquid ^{4}He (Ref. 10). The curves are calculated. The clamping field is $E_\perp=V/0.318$.

sult is that the expectation value of the image field, $\langle Qe/z^2\rangle_l$, had values of ~3.5 kV/cm, 430 V/cm, and 130 V/cm for $l=1$, 2, and 3, respectively, so that fields $E_\perp \approx 100$ V were not small in comparison.

The values found by Grimes *et al.*[10] for $dF_{12}/dE_\perp$ and $dF_{13}/dE_\perp$ turned out to be ~10% higher than those given by Eq. (9), if the wave functions in (6) are used to find the expectation values. When the finite barrier height V_0 is taken into account, however, and the image potential is adjusted to match the calculated value of $F_{12}(0)$ with the measured value, the calculated and measured transition frequencies are found to agree over essentially the entire range of $E_\perp$ studied (Fig. 3).

It is clear from the foregoing that in turning from liquid ^{4}He to ^{3}He, but retaining the hydrogen-like model, we must change the effective charge to correspond to the smaller value[12] $\varepsilon_3 = 1.04276$ for ^{3}He. The energies are accordingly reduced by a factor of 1.78 from those for ^{4}He, and the characteristic distances are increased by a factor of 1.33. Measurements by Volodin and Édel'man[13] confirm this conclusion: The transition frequencies turn out to be $F_{12} = 69.8 \pm 0.15$ and $F_{13} = 83.15 \pm 0.25$ GHz, in approximate agreement with the values 67.6 and 80.1 GHz, respectively, which can be calculated from the spectrum in (5). The change in the transition frequencies upon the imposition of an electric field is described well by Eq. (9) (Fig. 4) at small values of $E_\perp$.

As in the case of ^{4}He, the transition frequencies are slightly higher than the calculated values. According to the model discussed by Grimes *et al.*,[10] the ratio of the frequency shifts for the $1 \to 2$ and $1 \to 3$ transitions is independent of the particular properties of the liquid, having the value 208/189 = 1.10. For electrons above ^{4}He, according to Ref. 10, the ratio is $\delta F_{12}/\delta F_{13} = 1.08 \pm 0.05$. For ^{3}He, this ratio is 1.4 ± 0.2, and the comparatively high value here casts doubt on the applicability of the model.

When we compare the relative frequency shift $\delta F_{1l}/F_{1l}$, averaged for the $1 \to 2$ and $1 \to 3$ transitions, we find it to be 1.40 ± 0.15 times higher for electrons above ^{4}He than above ^{3}He. According to the model of Grimes *et al.*,[10] this ratio should be 1.33, in accordance with the ratio of the distances from the electron to the liquid surface in the two cases, if the surface properties of liquid ^{3}He and ^{4}He are the same. It can thus be concluded that there are no major differences in the physical properties of the surfaces of at least these two liquids. If we adopt the theoretical value[1,14] $V_0 = 0.9$ eV for the barrier height for ^{3}He, we find $\beta_3 = 1.25 \pm 0.15$ Å (Ref. 13), which is essentially the same as β_4.

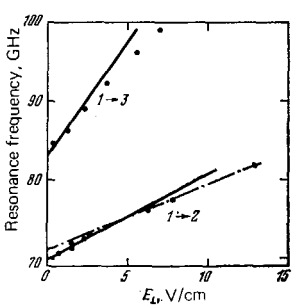

FIG. 4. Dependence on the retarding potential of the frequencies of the $1 \to 2$ and $1 \to 3$ transitions in the spectrum of electrons trapped above liquid ^{3}He (Ref. 13). The solid curves show the Stark shift calculated from the hydrogen-like model.

TABLE I. Characteristics of the electrons trapped above condensed cryogenic dielectrics.[14]

Substance	Phase state	10^3Q	V_0, eV		E_b, meV	$1/\gamma_0$, Å
			Theory	Experiment		
^{3}He	Liquid	5.2	0.9		0.39	100
^{4}He	Liquid	6.9	1.30	1.0±0.2	0.69	76
Ne	Liquid	22	0.47		11.5	24
	Solid	27	0.61		17.5	19
H_2	Liquid	26	2.2	0.3±0.2	11.5	20
	Solid	32	3.3		16.7	17
D_2	Liquid	31	3.1		16	17
	Solid	36	4.4		22	15

At the beginning of this section we mentioned that the electron motion along the surface was free motion. This assertion has been tested experimentally in a study of cyclotron resonance. If a static magnetic field H is applied perpendicular to the surface of liquid helium, it quantizes the motion along the surface; the energy spacing of the resulting Landau levels is $\hbar\Omega = \hbar eH/mc$. Measurements carried out at low temperatures, $T \approx 0.4$ K, at which the relative width of the cyclotron-resonance line is small, $\Delta H/H \approx 10^{-3}$, show that in the limit $E_\perp \to 0$ the electrons trapped above ^{4}He have a mass m which agrees within $\sim 10^{-4}$ with the free-electron mass.[15,16]

The two-dimensional nature of the electron motion can perhaps be seen most clearly in a study of the cyclotron resonance in a field H imposed at some angle with respect to the normal to the surface, **N**. Since the electron orbits in the magnetic field lie in the plane of the surface, the quantization of the motion of these electrons is determined by only that component of the field H which is directed along **N**. In this case we have $\Omega = eH\cos(\sphericalangle \mathbf{H}, \mathbf{N})/mc$, in other words, the effective mass is $m^* = m/\cos(\sphericalangle \mathbf{H}, \mathbf{N})$. This dependence has been found experimentally first in Ref. 17 and then in Ref. 15.

3. SUITABLE SYSTEMS FOR STUDY

Liquid helium is not the only dielectric with which electrons can form the bound states described in Sec. 2. In the very first papers which appeared on the subject, Cole and Cohen[1,14] pointed out several other dielectrics which had the necessary properties (see Table I).[1)] Electrification of the surface of liquid ^{4}He was observed by Sommer[18] even before a theory had been derived for the effect. The properties of electrons above ^{4}He have been studied in many papers. For other dielectrics, experiments along this line have been begun comparatively recently.

The trapping of electrons above liquid ^{3}He was first

[1)]Solid ^{3}He and ^{4}He are omitted from this table; they could be bounded by only an extremely dense gas or a liquid.

observed by Édel'man.[19] The cyclotron resonance of electrons above ^{3}He was studied in Ref. 20, and transitions in a hydrogen-like spectrum were observed in Ref. 13.

Observation of electrons trapped above liquid hydrogen[21] and solid neon and hydrogen[22] has recently been reported. The electrons above solid hydrogen are particularly interesting because of Khaĭkin's suggestion that large-radius negative hydrogen ions may exist.[23] The binding energy of the electron in such an ion would vary from ~17 MeV as the ion radius tended toward infinity to ~1 eV as the radius approached atomic dimensions.

Another system which may be of interest would be the electrons trapped above a film of superfluid helium on a flat substrate. This system has been studied theoretically in some detail by Shikin and Monarkha.[7] For an electron above a film of liquid helium of thickness d, the potential in (1) should be replaced by

$$\varphi(z) = -\frac{Qe^2}{z} - \frac{Q_u e^2}{z+d}, \tag{10}$$

in a first approximation, where we are ignoring the difference between ε_{He} and 1, $Q_{II} \approx (\varepsilon_{II}-1)/4(\varepsilon_{II}+1)$, and ε_u is the permittivity of the substrate. Expanding (10) in a series in terms of the small quantity z/d, and discarding the z-independent term, we find

$$\varphi(z) = -\frac{Qe^2}{z} + \frac{Q_u e^2}{d} z. \tag{11}$$

The substrate thus leads to an effective "clamping" field $E_{eff} = Q_u e^2/d$. For a typical film thickness ~400 Å, E_{eff} varies from ~400 V/cm for a substrate of solid H_2 to ~3 kV/cm for a metal substrate ($\varepsilon_u \to \infty$).

Experimental evidence for the existence of localized electron states above a helium film was found by Rybalko and Kovdrya,[24] who observed a slow return of electrons to the free surface of liquid helium after a brief removal of the clamping field. The time required for the electrons to return was of the order of several minutes. Volodin *et al.*[25] have found convincing evidence for the presence of trapped electrons above a film. Their apparatus is shown schematically in Fig. 5. Electrons are furnished by an electric discharge in a gas near the sharp point of the discharge gap, 1. A constant electric field $E_\perp$ is applied between a cylindrical copper cup 2 and the plane spiral coil 5 of the rf measuring circuit (resonant frequency ~3 MHz). The circuit lies inside an inverted cylindrical glass cup with a flat bottom (4).

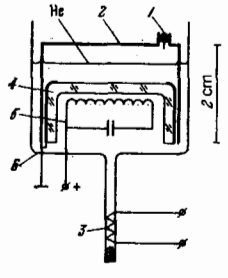

FIG. 5. Apparatus used to observe electrons above a film of liquid ^{4}He (the notation is explained in the text).[25]

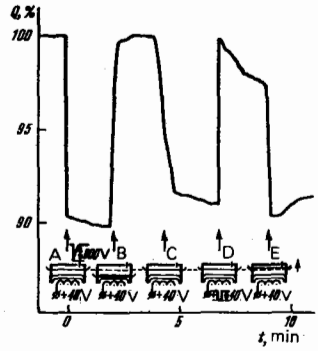

FIG. 6. Changes in the quality factor of the circuit in the apparatus in Fig. 5 during the events described in the text (from Ref. 25).

The apparatus is enclosed in a glass vessel 6, which is held above the liquid helium level in a cryostat. The helium is added to the vessel by means of the thermomechanical effect which occurs when the heater 3, in a capillary, is turned on; the helium level is adjusted by adjusting the heater power.

After a brief discharge (~0.1 s), the quality factor of the circuit, Q_c, falls off (from an initial value $Q_0 \approx 300$) because energy is absorbed by the electrons trapped above the helium (Fig. 6A). The decrease, $\Delta Q = Q_0 - Q_c$, is proportional in first approximation to the surface electron density n and can thus serve as a measure of the surface charge. The maximum surface charge density is determined by $E_\perp$:

$$n_{max} = \frac{E_\perp}{2\pi e}. \tag{12}$$

When the liquid level is lowered below the bottom of cup 4, the quality factor of the circuit resumes the value Q_0 (Fig. 6B); when the level is raised to its previous position, Q_c decreases again, showing that there are electrons above the free surface of the liquid (Fig. 6C). If the film of superfluid helium is destroyed by a temperature increase during the time between experiments B and C, the quality factor remains high after the liquid level is restored, and the dielectric turns out to be charged. These experiments demonstrate the existence of surface electron states above a helium film wetting a glass surface. The electron mobility above the film is lower than that above the surface of liquid helium by a factor of at least 10^3.

The next experiment demonstrates the existence of electron states above a film of superfluid helium which is wetting a metal surface. The brief removal of the clamping field causes a rapid escape of electrons from the surface, which is followed by a slow charging of the surface, over several minutes (Fig. 6D). When the helium level is raised to a small height, ~0.01 cm, the charge is completely restored (Fig. 6E). The charging of the surface in experiments D and E can be attributed to the runoff of surface electrons from above the helium film wetting the inner surface of metal cup 2 to the surface of the liquid. This runoff is caused by the electric field component along the film, $E_\parallel$, and by the fact that the electrons are rapidly "washed away" as the liquid level is raised. From the lateral surface area

of the cup and the amount of charge "washed away" in experiments like E, Volodin *et al.*[25] estimated the charge density above a helium film on a metal surface to be $n \approx (1-2)\cdot 10^{10}$ cm^{-2}. This value agrees well with our calculation of the maximum electron density, found by requiring that the negative energy of interaction of an electron with its own image charge and with those of its neighbors should balance the positive energy of its interaction with neighboring electrons. If it is assumed that the electrons form a square lattice on the film surface (this assumption will obviously have only a slight effect on the ultimate result), the value $n \approx (0.4/d)^2 \approx 10^{10}$ cm^{-2} is found. A similar runoff of electrons from a film onto a free helium surface was also observed in Ref. 26.

4. STABILITY OF THE CHARGED SURFACE

Limits are set on two quantities of some interest—the maximum possible electron density and the maximum clamping field—by a macroscopic instability of the charged liquid surface and by electron tunneling through the potential barrier.

The tunneling probability can be estimated from the semiclassical expression[27]

$$w \propto \exp\left(-\frac{2}{\hbar}\int_0^{V_0/eE_\perp} \sqrt{2m(V_0 - eE_\perp z)}\,dz\right) = \exp\left(-\frac{4}{3\hbar}\frac{V_0}{eE_\perp}\sqrt{2mV_0}\right). \quad (13)$$

Substituting $V_0 = 1$ eV, we find that the tunneling probability is low[28] for $E_\perp \lesssim 10^4$ esu.

At much lower values of $E_\perp$ there is a macroscopic instability of the charged surface. The reason is that, as the surface is deformed, the clamping field drives the highly mobile electrons to surface troughs, where they concentrate and intensify the deformation.

Gor'kov and Chernikova have studied the stability problem.[29,30] The equations derived in Ref. 30 for the spectrum of surface vibrations can be written as follows for the case in which the liquid is deep:

$$\omega_q^2 = \frac{q}{\rho}\left[\rho g + \sigma q^2 - \frac{q}{2\pi}(E_\perp^2 + 4\pi^2 n^2 e^2)\right]; \quad (14)$$

where ρ and σ are the density and the surface tension of the liquid, ω_q and q are the angular frequency and wave vector of the vibrations and $E_\perp$ and n are the clamping field and the surface electron density. Equation (14) holds if the vibration wavelength satisfies $\lambda = 2\pi/q \gg n^{-1/2}$. At the maximum charge $n_{max} = E_\perp/2\pi e$, which corresponds to complete shielding of the electrostatic field above the liquid, for the given $E_\perp$, we easily find from (14) that an instability can occur ($\omega_q^2 < 0$) at $q_0 = \sqrt{\rho g/\sigma}$ if

$$n^2 > n_{crit}^2 = \frac{\sqrt{\rho g \sigma}}{2\pi e^2}, \quad (15)$$

or

$$E_\perp^2 > E_{\perp\,crit}^2 = 2\pi\sqrt{\rho g \sigma}.$$

For ^{4}He in the limit $T \to 0$ we find $n_{crit} = 2.25\cdot 10^9$ cm^{-2} and $E_{\perp crit} = 2.03$ kV/cm. For $n \ll n_{max}$ (but $n \gg \rho g/4\pi^2\sigma \approx 10$ cm^{-2}) the critical field is higher by a factor of $\sqrt{2}$.

For a thin liquid layer, i.e., for $q_0 d \ll 1$, with complete shielding of the field above the surface, the vibration spectrum is[30]

$$\omega_q^2 = \frac{q^2 d}{\rho}\left(\rho g + \sigma q^2 - \frac{4\pi n^2 e^2}{d}\right). \quad (16)$$

In this case there is an instability with respect to long-wave vibrations ($q \to 0$) at

$$n_{crit}^2 = \frac{\rho g d}{4\pi e^2}, \quad (17)$$

or

$$E_{\perp\,crit}^2 = \pi\rho g d.$$

Equation (17) naturally holds for large values of d, at which Van der Waals forces can be neglected. For thin films, we must replace g in (16) and (17) by $f = 3gd_0^3/d^4$, where d_0 is the equilibrium film thickness at a distance 1 cm above the helium level.[31] For n_{crit} we find

$$n_{crit}^2 = \frac{3\rho g}{4\pi e^2}\left(\frac{d_0}{d}\right)^3. \quad (18)$$

With $d = d_0$, we find $n_{crit}^2 = 1.4\cdot 10^{10}$ cm^{-2}. Equation (18) gives us only an approximate value of n_{crit} for thin films, since it ignores the circumstance that the distance between electrons is greater than the film thickness.

The critical density has been measured by Rubalko and Kovdrya.[14] They found values in approximate agreement with those given by Eq. (15), but the temperature dependence turned out to be stronger than the $\sigma^{1/4}$ dependence which we would expect on the basis of the theory. Since the experimental procedure was not described in detail in Ref. 24, it is difficult to explain the reason for the discrepancy. It may be that the helium level dropped as the measurement cell was heated, because of vaporization, and the vapor density increased greatly.

Volodin *et al.*[32] studied in detail the instability mechanism in an electric field. The apparatus used in their experiments, carried out at $T \approx 1.3$ K, is shown schematically in Fig. 7. The electron source is a tungsten filament, 1. The voltage which creates the field $E_\perp$, which holds the electrons on the helium surface 2, is applied to the plates of a capacitor. The positively

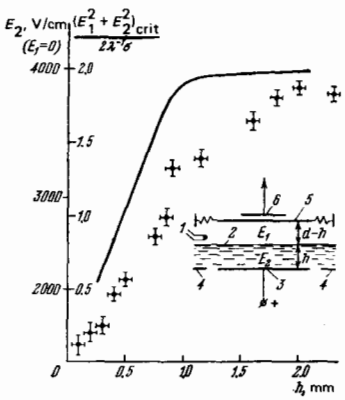

FIG. 7. The critical parameter as a function of the depth of the liquid layer, d (Ref. 32). The inset at the right shows the apparatus used to observe the instability of the charged helium surface.

charged lower plate, 3, is surrounded by a guard ring 4. The grounded upper plate, 5, is suspended on springs and can be moved vertically by the field E_1 so that the gap between this plate and the charged helium surface can be changed. The position of this upper plate is measured with a capacitor pickup, 6, and is taken as a measure of the field. The level of the superfluid helium in the capacitor is adjusted by exploiting the thermomechanical effect. The distance between the plates, h, is set at various values in the range 1–5 mm. The apparatus is placed in an optical cryostat. The dynamic effects are studied by high-speed motion-picture photography (up to 4000 frames/s).

At a certain initial helium level d_0, and at the voltage U_0 applied to the capacitor, electrons are emitted from the cathode, 1, which is turned on for a time ~0.1 s. The appearance of a surface charge is seen in a total shielding of the field above the helium surface, i.e., $E_1 = 0$. Then the critical conditions for the charged helium surface are achieved either by slowly lowering the helium level d or by raising the voltage U. The field E_1 is measured as a function of whichever parameter is varied. At the same time, the surface and volume of the liquid helium are monitored by high-speed motion-picture photomicrography.

The experimental results show that, when critical conditions are reached at the helium surface, capillary—gravitational waves are excited with an amplitude ~0.5 mm, and the surface charge disappears in a short time, ~0.1–0.3 s. These results imply a "severe" instability.[29,30]

Figure 7 shows the measured dependence of the critical value $(E_1^2+E_2^2)_{\text{crit}}$ on the helium level d. These experimental results agree satisfactorily with the calculation by Chernikova[30] (the heavy curve). The change in the nature of the dependence at $d \approx 1$–1.5 mm corresponds to the transition from an instability with respect to long-wave perturbations to an instability with a characteristic parameter equal to the capillary constant. This conclusion is confirmed by an analysis of the motion pictures: At $h \lesssim 0.6$–0.7 mm, the attainment of critical conditions is accompanied by the excitation of vibrations of the helium surface with wavelengths of the order of the dimensions of the capacitor plates, while at $d \gtrsim 1.5$ mm the wavelengths are of the order of the capillary length, ~0.5 mm. The motion pictures show the escape of electrons from the helium surface. Figure 8 shows four frames. The frame at the top shows a homogeneous and stable surface. The flat, equilibrium, charged helium surface is 0.2 mm below the helium level outside the capacitor because of electrostatic forces; both levels can be seen in this frame. When the instability occurs, and surface waves grow, sharp depressions appear at the wave troughs (frame 2 in Fig. 8). Bubbles from 0.05 to 0.3 mm in size are created in these sharp depressions (frame 3) and subsequently sink into the helium (the last frame). When a bubble reaches the bottom (the positive plate of the capacitor), it either collapses or floats back up, depending on its size: Bubbles 0.05 mm in diameter collapse in 10^{-4} s, while the large bubbles collapse in

FIG. 8. Successive motion-picture frames showing the excitation of oscillations on a flat ^{4}He surface (frame 1). 2) Instability; 3) formation of charged bubbles or "bubblons"; 4) the bubblons sinking into the helium.[32]

10^{-3} s, managing to float back up in the meantime.

The observations can be explained by arguing that each bubble is a multiply charged negative ion (with 10^7–10^8 electrons), or "bubblon," in the superfluid helium. The bubblon moves toward the anode and discharges when it gets there; the gas-filled bubble which remains collapses. Setting the electrostatic pressure inside the bubblon equal to the capillary pressure, we find an estimate of the bubblon radius:

$$r = \left(\frac{N^2e^2}{16\pi\sigma}\right)^{1/3} \approx 10^{-2} \text{ cm},$$

where N is the number of electrons in the bubblon, which is determined from the total surface charge and the number of bubblons required to discharge the surface (20–100). Because of the electrostatic interaction, the electrons in the bubblon form a two-dimensional layer near the liquid surface with an electron density 10^{11}–10^{12} cm^{-2}.

The small-diameter (0.05-mm) bubblons move through the liquid helium in a field $E = 1$ esu at a velocity of 10^4 cm/s, which corresponds to viscous Stokes motion. The time taken to reach the bottom is 10^{-3} s, which is much longer than the relaxation times of the electrical and elastic inhomogeneities in the bubblon dimensions.

Shikin[33] has studied the stability of multielectron bubbles in helium. He has shown that spherical bubblons with the properties found above are stable with respect to tunneling, the gravitational instability, and the deformation instability.

The instability and the spectrum of electrocapillary waves were also studied by Wanner and Leiderer,[34] who examined the trapping of electrons at a ^{4}He–^{3}He interface. Although the properties of the electrons themselves are quite different in this case from those for the electrons above a free helium surface, the dif-

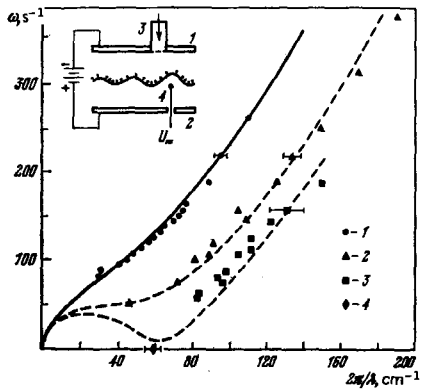

FIG. 9. Frequency of the electrocapillary waves as a function of the wave vector for $E_\perp$(V/cm) = 111 (1), 1000 (2), 1119 (3), and 1145 (4). Solid curve-wave spectrum of the uncharged surface; dashed curves-calculated for the corresponding charge density. $T = 0.567$ K. Inset at upper left: Apparatus used to measure the spectrum of electrocapillary-gravitational waves at an interface in a ^{3}He–^{4}He solution.[34] 1,2) Capacitor plates; 3) electron source; 4) electrode exciting oscillations of the interface (shown by the solid curve), observable in scattered light.

ferences are not important from the stability standpoint. Wanner and Leiderer[34] placed an electrode near the interface (Fig. 9) and applied an alternating voltage to it to excite electrocapillary waves. These waves were monitored by an optical arrangement. The wave spectrum, shown in Fig. 9 for various surface charge densities, is in excellent agreement with the theory.

Because of the significant viscosity of ^{3}He, which damps the waves, Wanner and Leiderer[34] were able to observe the predicted[31] formation of a spatially inhomogeneous state at $E_\perp > E_{\perp crit}$. A stationary hexagonal structure appeared at the interface, with a period equal to the capillary constant (Fig. 10). In later experiments, they observed a similar hexagonal structure for electrons above liquid ^{4}He at 4.2 K, at which the viscosity of helium is quite high.[35]

No special study has been made of the stability of charged surfaces of liquid ^{3}He and H_2, but it has been mentioned[20,21] that the critical values of the clamping field and the charge density are approximately equal to

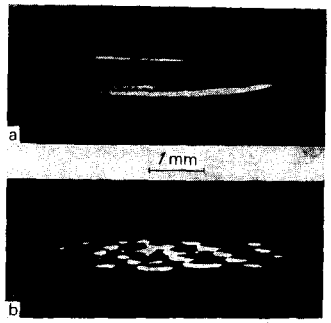

FIG. 10. a) Deformation of the interface at $E_\perp = 1120$ V/cm. The deformation is observed from below at an angle ~6° (the bright elliptical feature is caused by reflection from the annular edge of the charged region, being pressed downward; b) evidence of a steady-state periodic structure as $E_\perp$ is increased to 1160 V/cm ($T = 0.567$ K) (Ref. 34).

those expected theoretically in these cases.

There has been no study of the stability of charged surfaces of solid dielectrics, for example, H_2. Since the breakdown voltages of solid dielectrics are usually of the order of megavolts per centimeter, it can be expected that in this case $E_\perp$ and n for ideal crystals will be limited by tunneling and values $n \approx 10^{13}$ cm^{-2} can be reached, according to (13).

5. COLLECTIVE EFFECTS IN THE ELECTRON SYSTEM. WIGNER CRYSTALLIZATION

Because of the upper limit on the density of electrons above liquid helium (~$2 \cdot 10^9$ cm^{-2}), the Fermi-degeneracy temperature for these electrons is always low,

$$kT_F = \frac{p_{||}^2}{2m} = \frac{\pi\hbar^2 n}{m} \leqslant 0.01 \text{ K}. \tag{19}$$

On the other hand, the electron–electron Coulomb interaction is substantial:

$$V = \frac{e^2}{r} = e^2\sqrt{\pi n} \leqslant 100 \text{ K}. \tag{20}$$

On this basis, Crandall[36] has suggested that the surface electrons should become ordered in a two-dimensional lattice, thereby forming a Wigner crystal. The phase transition would occur when the ratio of the potential and kinetic energies per electron reaches the value[37]

$$\frac{V}{kT} = \Gamma, \tag{21}$$

where Γ is a constant, having the value $\Gamma = 77$ according to the calculation of Nagai and Onuki.[38] A similar value, $\Gamma = 95$, has been found by Hockney and Brown[39] in a computer simulation of the phase transition in a system of 10^4 particles.

The kinetic energy of the electrons also includes the energy of the zero-point vibration, which is of the same order of magnitude as the Fermi energy. Since this energy increases in proportion to n, according to (19) and (20), while the potential energy increases only in proportion to $\sqrt{n}$, it would be possible in principle to satisfy (21) at $T = 0$ by raising the density; in other words, it would be possible to arrange "cold melting" of the crystal.[37] However, numerical calculations based on (19) and (20) show that cold melting is not possible in this particular case. A density of even $n \approx 10^{11}$ cm^{-2}, which corresponds to the density in bubblons, would be far too low for cold melting. It is possible that this effect could occur for the electrons above a film of superfluid helium on a metal substrate, where the Coulomb interaction between the electrons, with their high density, would be significantly weakened by the shielding resulting from the nearby metal.[40]

Shikin and Monarkha[7,41] have shown that the deformation of the liquid surface beneath an electron leads to a further gain in potential energy upon crystallization. At the values of $E_\perp$ attainable above liquid helium, however, this additional energy is much smaller than that in (20), and it could apparently have no significant effect on the phase state of the electrons.

A question closely related to Wigner crystallization is the spectrum of collective oscillations of the elec-

tron system. According to Refs. 36 and 37, waves of two types can propagate in a two-dimensional system of electrons. The spectrum of longitudinal waves with $\lambda = 2\pi/q \gg h, d$ (d is the depth of the liquid, and h is the gap between the capacitor plates) is

$$\omega_L^2 = \frac{2\pi e^2 nq}{m}. \tag{22}$$

The existence and spectrum of these waves are independent of the phase state. The longitudinal waves in (22) are an analog of plasma waves, which are a well-known effect in the three-dimensional case. Their spectrum begins at $q = 0$ with the plasma frequency $(4\pi Ne^2/m)^{1/2}$, where N is the volume number density of electrons. There are differences in the properties of the longitudinal waves because the Coulomb interaction of two charged planes in the three-dimensional case does not depend on the distance between these planes, while the interaction of two charged filaments falls off with increasing distance. As q is reduced, the wave frequency thus decreases.

The transition to a crystalline state raises the possibility that transverse waves will propagate. At small values of q, they would have a linear spectrum (Ref. 36):

$$\omega_T = c_\perp q, \tag{23}$$

where $c_\perp^2 = 0.269e^2/mr$ for a triangular lattice.[37]

The application of a magnetic field $\mathbf{H} \| \mathbf{N}$ leads to collective oscillations with a spectrum[42]

$$\omega_\pm = \frac{1}{2}[\omega_T^2 + \omega_L^2 + \Omega^2 \pm \sqrt{(\omega_T^2 + \omega_L^2 + \Omega^2)^2 - 4\omega_T^2\omega_L^2}], \tag{24}$$

where Ω is the cyclotron frequency. We see that Eq. (24) goes over into (22) and (23) in the limit $H \to 0$. In the limit $q \to 0$ we find from (24)

$$\omega_+ = \Omega + \frac{\omega_L^2}{2\Omega} = \Omega + \frac{\pi e^2 nq}{m\Omega}, \qquad \omega_- = \frac{\omega_T\omega_L}{\Omega}. \tag{25}$$

Crandall[38] worked from the wave spectrum in a two-dimensional Wigner crystal to calculate the rms displacement amplitude of the electrons, $\langle r^2 \rangle$. The result found for an unbounded crystal was $\langle r^2 \rangle \to \infty$; i.e., long-range order could not exist in such a crystal even in the limit $T \to 0$. According to a computer simulation by Hockney and Brown,[39] there is only short-range order near the transition temperature in the system, and the "crystal" breaks up into small domains.

Many theoretical papers have been published on the ordered state of a two-dimensional system of electrons; a thorough examination of these papers goes beyond the scope of the present review. In contrast, very few experimental papers have appeared on many-electron interactions.

Grimes and Adams[43] have observed the excitation of longitudinal standing waves [Eq. (22)] in rectangular cells with dimensions $a \times b = 12 \times 12$ mm with $q_x = n\pi/a$ and $q_y = m\pi/b$ (Fig. 11). The spectrum calculated for these waves, with allowance for the shielding effect of the electrodes,[44] agrees with the measured spectrum (Fig. 12).

Zipfel *et al.*[45] carried out an experiment which demonstrated a correlation in the electron system. They studied the width of the $1 \to 2$ transition line in the spectrum in (5) as a function of a magnetic field imposed parallel to the surface of liquid helium. The magnetic field leads to a Lorentz force directed along the normal to the surface; this force is equivalent to an electric field $v_x H/c$. Since there is a velocity distribution, which is described for a free-electron gas by $\exp(-mv_x^2/2kT)$, the Lorentz force broadens the resonant line (Fig. 13). This broadening, however, is less than that which should be observed for an electron gas. As the surface density of electrons increases, the effect of the magnetic field diminishes.

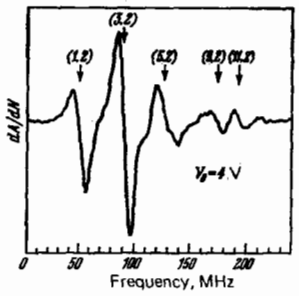

FIG. 11. Frequency dependence of the derivative with respect to the surface electron density of the absorption of an rf signal transmitted through a cell 19×12 mm in area, 1.8 mm high, partially filled with ^{4}He (Ref. 43). The order of the interference of plasma waves is shown in parentheses. $T \approx 0.5$ K.

This effect can be explained in the following manner. If the characteristic frequency satisfies

$$\Delta\omega = 2\pi \frac{v_x H}{c} \frac{dF_{12}}{dE_\perp} \ll \frac{1}{\tau},$$

where τ is the collision time in the system of electrons, then the line is narrowed by a factor of $\Delta\omega\tau$ because of the change in the state of the electron; this effect is analogous to the familiar NMR effect. According to the measurements (Fig. 13), the characteristic time for an electron density $\sim 2 \cdot 10^8$ cm^{-2} is $\tau = 1.5 \cdot 10^{-11}$ s, in good correspondence with the period of the oscillation of an electron about its equilibrium position.[45]

Attempts to observe the ordered state experimentally run into substantial difficulties. Observation of light diffraction, as proposed in Ref. 36, is complicated by

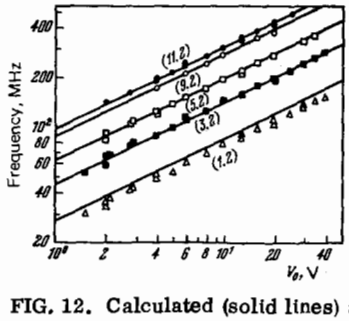

FIG. 12. Calculated (solid lines) and measured frequencies of the standing-wave resonances of longitudinal plasma oscillations for various values of the retarding potential.[43] For this particular case, the surface density is $n = 8.6 \times 10^6$ V cm^{-2}; $T \approx 0.5$ K.

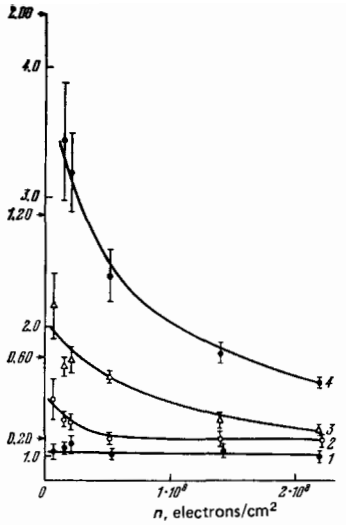

FIG. 13. Line width ΔF_{12} for the $1 \rightarrow 2$ resonance transition as a function of the electron density in a magnetic field H, normalized to $\Delta F_{12}(0) \approx 1.5$ GHz (Ref. 45). 1 – 4) $H = 0.20$, 0.60, 1.2, and 2.0 kG, respectively. The arrows beside the ordinate axis shows the value $\Delta F_{12}(H)/\Delta F_{12}(0)$ calculated for a gas of noninteracting electrons. ^{4}He, 1.2 K, $F = 225$ GHz.

the small cross section for photon scattering by both electrons and ions in liquid helium, which have characteristic dimensions $\sim 10^{-7}$ cm $\ll \lambda$. Furthermore, as Platzman and Fukuyama have pointed out,[37] the absence of long-range order should lead to a blurring of the Bragg reflection.

A study of Wigner crystallization on the basis of the conductivity of the two-dimensional system is complicated by the circumstance that in a homogeneous electric field and a magnetic field the electron–electron interaction does not itself affect the conductivity. In an inhomogeneous electromagnetic field it is a comparatively simple matter to excite and observe longitudinal waves with characteristic velocities $\sim 10^9$ cm/s (Ref. 43), but to observe transverse waves with a velocity $\sim 10^6$ cm/s—and thereby find unambiguous proof of crystallization—is a complicated experimental problem, which has yet to be solved.

Another consequence of the small value of v_{pl}/c is that the absorption occurs near the cyclotron frequency in a magnetic field, and the electron–electron interaction does not affect the position of the cyclotron resonance line[46] in (25), as has been confirmed experimentally.[20]

Monarkha and Shikin[41] have suggested observing crystallization on the basis of the particular features of the absorption of energy from an electromagnetic wave which is polarized perpendicular to the liquid surface; the absorption results from the excitation of capillary waves by the electron lattice. According to their calculation, the absorption coefficient α is

$$\alpha = \frac{8\pi}{c}\eta\frac{e^2}{\rho^2}\omega^2\sum_q q^3\frac{n_q^2}{|\omega^2-\omega_q^2+2i\omega\chi q|^2}, \qquad (26)$$

where n_q is the Fourier component of the electron density, $\omega_q^2 = (\sigma/\rho)q^3$, and q is one of the reciprocal-lattice vectors. For a triangular lattice, we would have

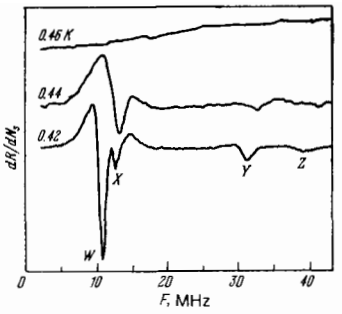

FIG. 14. Experimental traces demonstrating the appearance of plasma–ripplon resonances as the temperature is reduced, because of the crystallization of electrons in a triangular lattice.[48]

$|q|^2 = l\cdot 8\pi^2 n/\sqrt{3} = lq_0^2$, $l = 1, 3, 4, 7, 9, \ldots$; for a square lattice, $|q|^2 = l\cdot 4\pi^2 n$, $l = 1, 2, 4, 5, 8, \ldots$ $\chi = (\eta/\rho)q^2$, where η is the first viscosity coefficient of helium. Equation (26) predicts a resonant increase in α in the limit $\omega \rightarrow \omega_q$. Setting $n_q \approx n$, we estimate the absorption at resonance to be

$$\alpha \approx \frac{2\pi}{c}\frac{e^2n^2}{4\eta q}. \qquad (27)$$

Substituting $n = 10^9$ cm^{-2} and $3 \approx 30\mu P$ for ^{4}He at 1 K, we find $\alpha \approx 10^{-12}$. This value is too low for the effect to be observed.

Even for electromagnetic waves which are polarized along the surface, however, there should be a resonant absorption resulting from the interference of ripplons.[47] This effect was in fact exploited by Grimes and Adams[48] as a means for observing Wigner crystallization.

In their experiments, they studied the temperature dependence of the absorption of rf power by a system of electrons of density n trapped above liquid helium. They found clearly defined resonances in a narrow temperature interval against the background of an otherwise monotonic dependence (Fig. 14). The frequencies corresponding to resonances Y and Z agree within $\sim 2\%$ with the ripplon frequencies corresponding to the vectors of a triangular reciprocal lattice with $l = 3$ and 4. The behavior of W and X is more complicated: First, there are two resonances; their frequencies, 10.2 and 12.3 MHz, (for $n = 4.4\cdot 10^8$ cm^{-2}), are much lower than the frequency of ripplons with $q = q_0$, which is 15.1 MHz; and, finally, the positions of these resonances depend on both the clamping field and the temperature.

These features were explained by Fisher *et al.*,[47] who calculated the changes in the spectrum of ripplons resulting from their interaction with electrons. An electron forced toward the surface by the electric field forms a depression beneath itself (Section 8). A slowly moving electron will "drag" this depression along, furnishing an effective mechanism for energy transfer from electrons to surface vibrations and back. Since the velocity at which excitations propagate through the system of electrons is much higher than the velocity of a surface wave, this interaction leads to a renormalization of the ripplon spectrum: this renormalization turns out to be important at wave vectors $q \approx q_0$ and unimportant at $q^2 = 3q_0^2$, $q^2 \approx 4q_0^2$.

According to this theory, there are two resonances, W and X, instead of one because longitudinal plasma waves of various lengths can be coupled with the external rf field under these experimental conditions; the wavelengths are determined by the dimensions and configuration of the measurement cell. Since the change in the ripplon spectrum depends on the wave vector of the plasma waves, there is the possibility that several resonances will be observed. The $E_\perp$ dependence of the resonant frequency is quite understandable: As the clamping field is reduced, the binding of the electrons to the surface will weaken, and in the limit $E_\perp \to 0$ the resonant frequency should approach the frequency determined from the spectrum for "free" ripplons. This conclusion agrees with experiment.[48]

It can thus be considered an established fact that a phase transition to an ordered state corresponding to a triangular lattice occurs in the system of electrons (the resonant frequencies would be completely different for a square lattice). According to Ref. 48, the transition occurs at $\Gamma = 137 \pm 7$ at temperatures in the range 0.4–0.7 K; this value is not far from the value $\Gamma = 95$ which was calculated in Ref. 39.

Rybalko *et al.*[49] have reported observing a discontinuity in the field dependence of the electron mobility, $\mu(E_\perp)$, at $T \lesssim 0.3$ K, at a position which corresponds to the condition $\Gamma \approx 140$. They attribute this anomaly to Wigner crystallization. Monarkha[50] has calculated the mobility for this case.

6. INTERACTION OF THE ELECTRONS WITH VAPOR ATOMS

Surface electrons may interact with vapor atoms and with thermal vibrations of the dielectric surface. The relative importance of the effects of these interactions is very sensitive to the temperature and the clamping field. For example, the vapor density is comparatively high for ^{4}He at $T \gtrsim 1$ K and for ^{3}He at $T \gtrsim 0.4$ K, and collisions with vapor atoms dominate the scattering. At lower temperatures, the vapor density falls off exponentially and ceases to affect the electron dynamics.

If the vapor density is not too high, it will affect only the electron mean free path. If the temperature is low enough, and the clamping field high enough, that all the electrons are in the ground state, then the electron mobility μ is[14,17,51]

$$\mu_{2D} = \frac{e\tau}{m} = \frac{e}{\pi\hbar\sigma_s N}\left(\int_0^\infty \Phi_1^4\, dz\right)^{-1} = \frac{8e}{3\pi\hbar\sigma_s N\gamma}. \qquad (28)$$

Here σ_s is the cross section for the scattering of slow electrons by an atom [for He, $\sigma_s = 4.9 \cdot 10^{-16}$ cm^2; Ref. 52], N is the number of vapor atoms per cubic centimeter, and the wave function in (6) has been used in evaluating the integral. The two-dimensional mobility is lower than the electron mobility in the three-dimensional case, which is given by the classical formula

$$\mu_{3D} = 4e\,(3N\sigma_s\sqrt{2\pi mkT})^{-1} \qquad (29)$$

The ratio of these mobilities is

$$\frac{\mu_{2D}}{\mu_{3D}} = \frac{\sqrt{2kT/m}}{\sqrt{\pi}\,\hbar\gamma/2m}, \qquad (30)$$

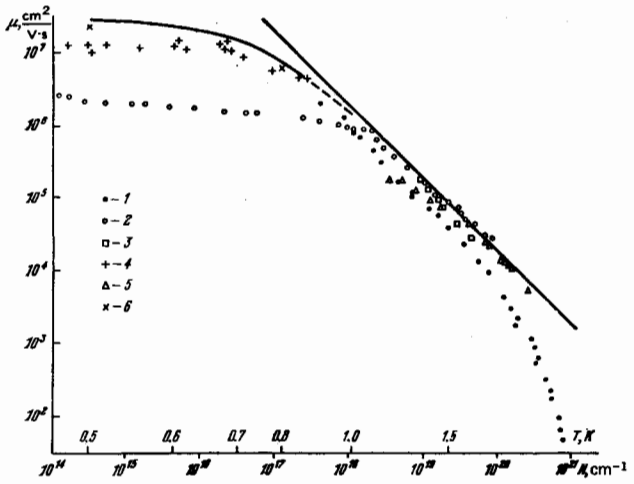

FIG. 15. Mobility of the electrons trapped above liquid ^{4}He as a function of the temperature T and the vapor density N. 1 – 5) Measurements; 1) based on the effect of the electrons on the mutual capacitance of the electrodes in the sonic frequency range[53]; 2) based on the loss caused in a megahertz-range rf circuit[54]; 3) based on the width of the cyclotron-resonance line at 23.5 GHz (Ref. 17); 4) based on the line width of resonance standing plasma waves in the frequency range 20 – 400 MHz (Ref. 43); 5) by a time-of-flight method (Ref. 55); 6) calculation of Ref. 60; straight line — calculation for scattering by vapor atoms; solid curve — results calculated in Ref. 61 for $T \lesssim 0.8$ K.

i.e., equal to the ratio of the thermal velocity to a quantity which represents the characteristic velocity of the electron in the potential well near the dielectric surface. For ^{4}He at $T \approx 1$ K, the ratio is $\mu_{2D}/\mu_{3D} \approx 0.15$.

Various methods have been used to measure the electron mobility above liquid helium at $T \gtrsim 1$ K: a method based on the quasistatic conductivity,[53,54] a time-of-flight method[55]; one based on the width of resonances of standing plasma waves[43]; and one based on the width of a cyclotron resonance line.[17] The results on $\mu(N)$ are shown in Fig. 15. For 10^{18} cm$^{-3} \leq N \leq 10^{20}$ cm^{-3}, the $\mu(N)$ dependence is linear, and the absolute values of μ, which are very sensitive to the calibration of the measurement apparatus for the methods other than the resonance methods, differ from the theoretical results [Eq. (28)] by no more than they differ from each other.

At $N \gtrsim 10^{20}$ cm^{-3} the mobility begins to fall off more rapidly than the rate of increase of N, because bound states of electrons with vapor atoms appear.[56] These states are beyond the scope of the present review.

The clamping field $E_\perp$ has comparatively little effect on the gas mobility. A decrease in τ by a factor of two has been observed as $E_\perp$ was increased to its critical value.[20] The reason for this effect is that the average image field for ground-state electrons in the case of ^{4}He, ~3.3 kV/cm, is higher than the critical field, ~2 kV/cm (Sections 2 and 4), so that the ground-state wave function changes only negligibly.

The scattering by vapor atoms determines the electron mobility above solid hydrogen[22] (Fig. 16). The apparent reason for the decrease in the electron mobility above liquid H_2 is the trapping of electrons as

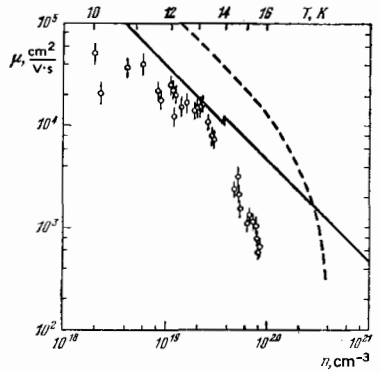

FIG. 16. Mobility of the electrons trapped above condensed hydrogen as a function of the temperature and the vapor density.[22] The line with the jog (at the melting point) shows results calculated for scattering by vapor atoms. The dashed curve shows $\mu(N)$ for electrons above ^{4}He (cf. Fig. 15).

the vapor density increases, just as in the case of helium.

Collisions with a gas also determine the width of the transition lines in the hydrogen-like spectrum at[10,57] $T \gtrsim 1$ K (Fig. 17). According to Grimes *et al.*,[10] the line width varies in proportion to the vapor density, and an extrapolation to $N=0$ leads to the finite value $\Delta_0\nu \approx 500$ MHz. Grimes *et al.*[10] attribute the residual width to the inhomogeneity of the electric field, $\Delta E_\perp / E_\perp \approx 1\%$, in the measurement cell. A fivefold change in $E_\perp$, however, does not change $\Delta_0\nu$, as it should. The comparison with theory in Refs. 10 and 57 demonstrates a satisfactory agreement, but one circumstance remains unclear: While a value ~1 GHz was found in Ref. 10 for the full line width (more precisely, for the distance between the extrema of the derivative, which is smaller than the width at half-maximum by a factor of $\sqrt{3}$) at $T \approx 1.2$ K, the same workers subsequently found[45] a much larger value, 1.4–1.7 GHz—more than twice the calculated value. Interestingly, for the primary scattering mechanism, involving collisions with vapor atoms, the line width for the $1 \to 2$ transition is essentially equal to the cyclotron-resonance line width.[10,17]

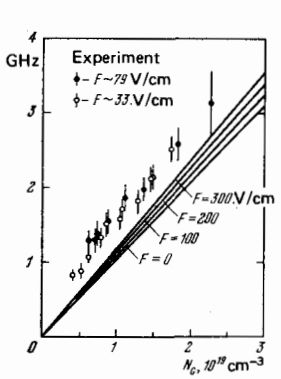

FIG. 17. Distance between the extrema of the derivative as a function of the ^{4}He vapor density for the resonance at the $1 \to 2$ transition, measured in Ref. 10. The lines show the calculations of Ref. 57 for various values of the clamping field.

7. ELECTRON SCATTERING BY THERMAL VIBRATIONS OF THE LIQUID SURFACE

As the temperature is reduced, and the vapor density falls off exponentially, the interaction of electrons with the liquid surface becomes increasingly more important. Two effects are seen: scattering by surface thermal vibrations and a deformation of the liquid beneath the electron, because of the force $eE_\perp$, which changes the electron dynamics.

Atkins[58] introduced the concept of ripplons, or elementary surface excitations. Their spectrum is the same as that of capillary waves, i.e., is described by [cf. (14)]

$$\omega_q^2 = \frac{\sigma}{\rho} q^3. \tag{31}$$

Scattering of electrons by ripplons was predicted theoretically by Cole,[14] whose results were subsequently corrected by Shikin and Monarkha.[59] According to that work, the collision frequency is[60]

$$\nu(p) = \frac{m}{2\pi\hbar^3} \int_0^{2\pi} d\varphi \, |\langle V_q \rangle|^2 (2N_q + 1)(1 - \cos\varphi), \tag{32}$$

where

$$N_q = \left(\exp\frac{\hbar\omega_q}{kT} - 1\right)^{-1} \approx \frac{kT}{\hbar\omega_q} \tag{33}$$

for the ripplons of importance here; $q = (2p/\hbar)\sin(\varphi/2)$, and p is the electron momentum. The interaction is described by the function

$$V_q = \sqrt{\frac{\hbar q}{\rho\omega_q}} \left\{ Qe^2 \frac{q}{z} \left[\frac{1}{qz} - K_1(qz) \right] + eE_\perp \right\}, \tag{34}$$

where $K_1(x)$ is the modified Bessel function. As Platzman and Beni[61] have pointed out, the value of qz at $T \lesssim 1$ K is so low that (34) can be expanded in a series in qz, and results accurate within ~10% can be calculated by retaining only terms of order lower than $(qz)^2$. (Within the same error, the result found in Ref. 61 for μ at $E_\perp = 0$ agrees with the value found by a computer calculation in Ref. 60. Similar results were found in Ref. 57.) Then it becomes a straightforward matter to integrate (33) and find[61]

$$\nu(p) = \frac{mkTe^2}{2\hbar\sigma p^2} \left\{ E_\perp^2 - E_\perp \frac{p^2 Qe}{\hbar^2} \left[2\ln\left(\frac{p}{4\gamma\hbar}\right) + 3 \right] + \left(\frac{p^2 Qe^2}{\hbar^2}\right)^2 A(p) \right\}, \tag{35}$$

with $A(p) \approx 1.22 + 2.67\ln(p/2\hbar\gamma) + 1.5[\ln(p/2\hbar\gamma)]^2$.

Knowing $\nu(p)$, we can calculate the electron mobility. In strong fields ($E_\perp \gtrsim 1$ kV/cm) at $T \approx 0.5$ K and with $\omega\tau = (\omega m/e)\mu \ll 1$ (Ref. 59) we have

$$\mu_{LF} = \frac{8\sigma\hbar}{meE_\perp^2}. \tag{36}$$

In the opposite limit, $\omega\tau \gg 1$, according to Ref. 61, we have

$$\mu_{HF} = \frac{4\sigma\hbar}{meE_\perp^2} = \frac{\mu_{LF}}{2}. \tag{37}$$

Figure 15 shows the results calculated for $\mu(T)$ in Refs. 61 and 60 for $E_\perp = 0$. Also shown there are the measurements of μ_{LF} (Ref. 54) and μ_{HF} in the limit $E_\perp \to 0$ (Ref. 43). While the agreement between theory and experiment can be judged completely satisfactory for the high-frequency mobility, the results calculated for μ_{LF} are an order of magnitude above the measured val-

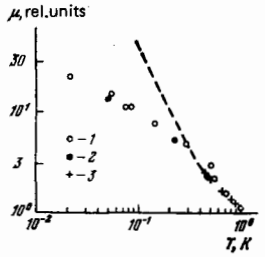

FIG. 18. Temperature dependence of the mobility of the electrons above ^{4}He, determined from the losses in an rf circuit.[62] 1, 2) Measurements at 12 and 25 MHz, respectively; 3) results of Ref. 54. The clamping fields lie in the range 10 – 50 V/cm; the density is $10^7 - 10^8$ cm^{-2}.

ue. The discrepancy becomes even worse at $T \lesssim 0.2$ K (Fig. 18).[62]

One reason for the discrepancy may be that the particular features of measurement of the mobility on the basis of the absorption of electromagnetic-wave energy in the case of electrons trapped above helium were not taken into account in Refs. 54 and 62. In contrast with three-dimensional conductors, for which closed currents can flow along the surface, so that the electric field leads to essentially no local changes in the electron density, there should be changes of this sort for the electrons trapped above a dielectric. If the density changes quite rapidly, as it does if $\psi = ne\mu/\omega R \gg 1$ (R is the characteristic dimension of the system), then the Coulomb field of the electrons will, to a significant extent, cancel the alternating external field, leading to a decrease in the high-frequency loss.

For the experimental conditions of Ref. 62, the value of ψ is ≈ 2–20, and the change in the electron density must be taken into account. Unfortunately, only an extremely brief description of the experiment was given in Ref. 62, and it is accordingly difficult to say to what extent this circumstance affected the results, which depend on the experimental geometry to a large extent. For strictly circular currents, for example, there would be no charge redistribution, and no correction at all would have to be made.

The $E_\perp$ dependence of μ_{HF} was measured in Ref. 43 for fields in the range $E_\perp \lesssim 200$ V/cm. It was found that $\mu_{HF} = 9.3 \cdot 10^{11}(230 + E_\perp)^{-2}$ cm^2/(V · s), within the experimental error of ~5%; this result is essentially the same as the calculated result.[61] Extrapolation to strong fields, $E_\perp \gg 230$ V/cm, leads to a result which agrees within ~10% with the value calculated from (37).

A cyclotron-resonance study[20] has revealed qualitative discrepancies between the theory of Refs. 60 and 61 and experiment. While Eqs. (36) and (37) predict that τ will be independent of both T and ω in strong fields $E_\perp$, the experiments of Ref. 20 show that the value $\tau = mc/e\Delta H$ found from the half-width of the cyclotron-resonance line, ΔH, is proportional to ω/T (Figs. 19 and 20). A qualitative explanation for the situation can be found by noting that the condition $\hbar\omega > kT$ holds under the experimental conditions here, so that only the one lowest Landau level is populated, and all the electrons have the same characteristic momentum $p^2 = e\hbar H/2c$. Thus the

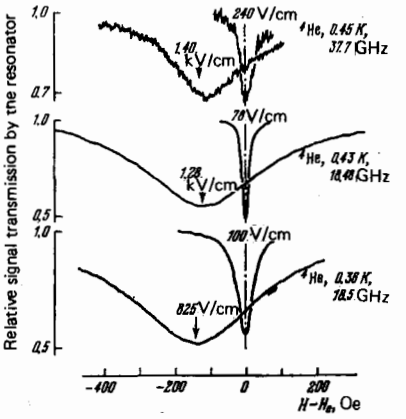

FIG. 19. Cyclotron-resonance signal under various experimental conditions, demonstrating the broadening and shift of the resonance with increasing clamping field.[20] H_0 is the cyclotron-resonance field for free electrons.[20]

collision frequency and its reciprocal, the relaxation time, are determined directly from (35) with this value of p^2. The value of $\Delta H \propto T/\omega\sigma$ found on the basis of these qualitative arguments agrees with experiment at large values of $E_\perp$ (Fig. 20), and this agreement is apparently not simply fortuitous, since a change in the electron density—not reflected in any way in the theory—leads to a significant change in ΔH. Judging from the relation $\Delta H(^3\text{He})/\Delta H(^4\text{He}) = \sigma_4/\sigma_3$, which holds at the maximum value of n, the behavior of $\Delta H(n)$ cannot be described by simply incorporating the electron–electron interaction, studied in Section 5. Dykman and Khazan[63] have developed a theory for cyclotron resonance which incorporates the electron–electron interaction, but they find a weaker dependence of the line width on $E_\perp(E^{5/4})$ and on $H(H^{1/2})$ than was found in Ref. 20.

As $E_\perp$ is reduced, the measured values of ΔH turn out to be an order of magnitude larger than those which follow from (35). Furthermore, there is a "descending" region of the dependence $\Delta H(E_\perp, n = E_\perp/2\pi e)$ (Fig. 21), while $\nu(p)$ is a monotonic function of $E_\perp$. This situation can be explained qualitatively on the basis that, as n increases, not all the scattering events

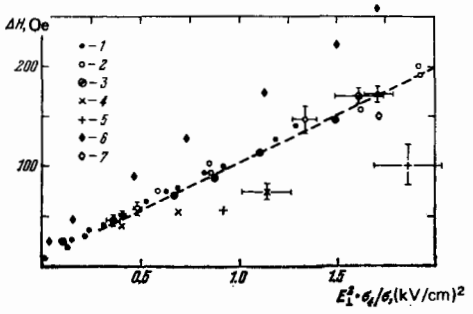

FIG. 20. Half-width of the cyclotron-resonance line, ΔH, as a function of the square of the clamping field (normalized to the surface tension).[20] 1, 2, 4 – 7—Electrons above ^{4}He; 3—above ^{3}He; 2—$f = 37.7$ GHz; otherwise—$f = 18.5$ GHz; 1 – 3, 6—$n = n_{max}$; 4, 5—$n \approx (0.2 - 0.3)n_{max}$; 1 – 5—$T = 0.4$ K; 6—0.74 K; 7—value of ΔH. (0.4 K)/(0.74 K) for case 6; dashed line—calculation from Eq. (35) with $p^2 = e\hbar H/c$.

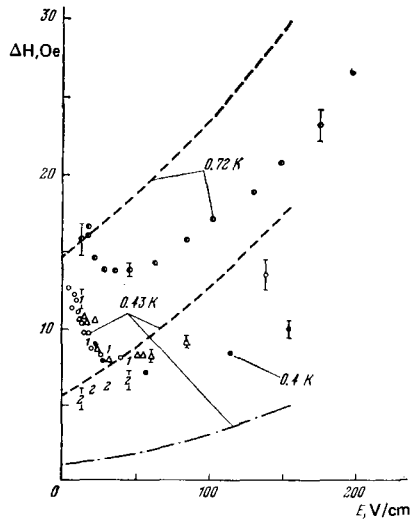

FIG. 21. The half-width of the cyclotron-resonance line, $\Delta H(E_\perp)$, for electrons above ^{4}He at the specified temperatures.[20] The various points for $T = 0.43$ K show experimental results obtained on different days. 1 and 2—Values of $\Delta_1 H$ and $\Delta_2 H$ obtained in the same experiment; dashed curve—twice the value of ΔH calculated from the mobility equation from Ref. 61; dot-dashed curve—from Eq. (35) with $p^2 = e\hbar H/c$.

allowed by momentum conservation can actually occur; the only ones which occur are those for which that change which is caused in the electron energy in the field of other electrons by a change $\sim\sqrt{c\hbar/eH}$ in the position of the center of the orbit is smaller than the ripplon energy. The value $E_\perp$ which follows from this condition is ~15 V/cm.

The electron–ripplon interaction at low temperatures should also determine the line width for transitions in the hydrogen-like spectrum in (5). The calculations of Ref. 57 yield the value $\Delta F_{1l} \approx 3$ MHz for $1 \to l$ transitions of the electrons above ^{4}He at $T \approx 0.4$ K; i.e., they yield a value an order of magnitude smaller than the half-width of the cyclotron-resonance line, ~30 MHz. In contrast, the value $\Delta F_{1l} = 450 \pm 120$ MHz was found in Ref. 20. Interestingly, this value is of the same order of magnitude as that found by extrapolating to zero vapor density in Fig. 17.

For electrons above ^{3}He at $T \approx 0.36$ K, the measured value is $\Delta F_{1l} \approx 1.6$ GHz (Ref. 20), which is again much larger than the half-width of the cyclotron-resonance line, determined in this case by scattering by the gas and having the value ~60 MHz. According to the results of Ref. 10 (Fig. 17), we would expect $\Delta F_{1l} \approx 60$ MHz for scattering by the vapor.

The measurements in Ref. 20 were carried out in a magnetic field ~6 kOe, directed normal to the liquid surface, but this field should apparently not affect[9] ΔF_{1l}. The fact that the line width is independent of the electron density implies that the broadening is not due to the electron–electron interaction.

In summary, the theory for electron–ripplon scattering requires further refinement, especially for weak clamping fields.

8. DEFORMATION LOCALIZATION

When a clamping field is imposed, the electrons press against the liquid surface, deforming it. As a result the electron dynamics undergoes a change. This subject has been studied theoretically in Refs. 64 and 65 (see also Ref. 7), where it was shown that the deformation can lead to electron trapping in a plane within a region with a characteristic dimension

$$L_\xi^2 = \frac{2\pi\sigma\hbar^2}{me^2E_\perp^2}; \tag{38}$$

we find $L_\xi \approx 2 \cdot 10^{-5}$ cm for $E_\perp = E_{\perp\text{crit}} \approx 2$ kV/cm. The energy gain in the bound state results from the decrease in the energy of the electron in the electric field as the electron drops along with the liquid. According to Ref. 7, this energy change is

$$\delta E = -\frac{e^2E_\perp^2}{4\pi\sigma}\left(\ln\frac{\alpha}{L_\xi\sqrt{0.89}} - 1\right) \tag{39}$$

($\alpha = \sqrt{\sigma/\rho g}$ is the capillary constant) or $\delta E \sim 0.1$ K at $E_\perp = E_{\perp\text{crit}}$. Then the formation of a "surface anion" should be observed only at temperatures $T \ll 0.1$ K, at which no experiments have yet been carried out.

As mentioned in Ref. 7, the appearance of surface anions should be facilitated by an external magnetic field, which if $\hbar\Omega > kT$ will automatically lead to a trapping of electrons in a region

$$L_H^2 = \frac{2\hbar c}{eH}, \tag{40}$$

or by Wigner crystallization (Section 5).

Surface anions should have quite unusual characteristics. In a low-frequency alternating field they would behave as if they were particles with a large mass and a correspondingly low mobility. This circumstance may furnish an explanation for the very low mobility, $\sim 10^{-1}$ cm^2/(V·s), of the electrons trapped above a film of superfluid helium. In this case, it is highly probable that surface anions will be formed by the effective clamping field of the substrate[7] (Section 3).

In high-frequency fields, e.g., in cyclotron-resonance experiments, the motion of the electron in the depression it forms at the surface is adiabatic, and the resonant frequency is higher than the cyclotron frequency; i.e., the effective electron mass is smaller than m (Ref. 46). This effect was first observed experimentally in Ref. 15. Cheng and Platzman[66] and Shikin[67] have calculated the frequency shift. An electron in a Landau ground state with a wave function

$$\psi_0 = \frac{1}{L_H\sqrt{\pi}} e^{-r^2/2L_H^2} \tag{41}$$

exerts a pressure $eE_\perp|\psi_0|^2$ on the liquid, deforming it. The deformation is described by the equation

$$\nabla_\parallel^2\zeta = \frac{eE_\perp|\psi_0|^2}{\sigma}, \tag{42}$$

where ζ is the change in the normal coordinate of the liquid surface. In a transition to the $n = 1$ state, the slowly varying surface deformation remains unchanged, so that perturbation theory can be used to calculate the associated correction to the cyclotron frequency:

$$\hbar\Delta\Omega = \int (|\psi_1|^2 - |\psi_0|^2)\, eE_\perp\zeta(r) \cdot 2\pi r\, dr. \tag{43}$$

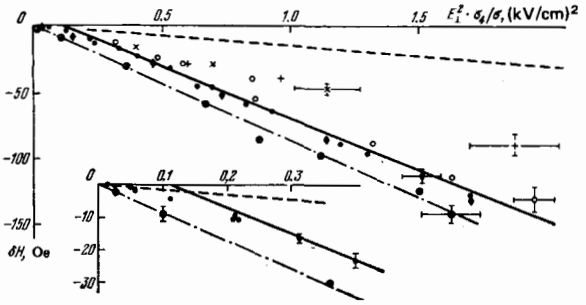

FIG. 22. Shift of the cyclotron resonance, δH, as a function of $E_\perp^2$ (Ref. 20). The notation is the same as in Fig. 20. Dashed line—Calculated from Eq. (45); solid and dot-dashed lines—drawn through the experimental points for ^{4}He and ^{3}He, respectively.

Calculations[66,67] yield

$$\Delta\Omega = \frac{e^2 E_\perp^2}{8\pi\sigma\hbar}, \tag{44}$$

or the shift of the resonance line in the field is

$$\delta H = -\frac{mecE_\perp^2}{8\pi\sigma\hbar}. \tag{45}$$

The same problem was studied in Ref. 63, where the result found for the frequency shift differed from that in (44) by a factor $kT/\hbar\Omega < 1$.

The measurements of Ref. 20 confirmed some qualitative conclusions which follow from (45): δH is independent of Ω, and it is a quadratic function of $E_\perp$ (Figs. 19 and 22). Here we have a ratio $\delta H(^3\text{He})/\delta H(^4\text{He}) \approx \sigma_4/\sigma_3$, as follows from the theory. Numerically, however, δH is above five times the value given by Eq. (45), and, in contrast with the theoretical predictions of Ref. 66, it depends on the electron density. This latter point may furnish a key to the problem: The electron–electron interaction leads to a further trapping of electrons. The calculations of Refs. 67 and 68 for the shift of the cyclotron-resonance line in the case $T = 0$ showed that the electron–electron interaction can lead to a value of δH approximately the same as that found experimentally. According to the theory, however, a $\delta H(\Omega)$ dependence appears, and the dependence on the clamping field is more complicated than a $E_\perp^2$ dependence.

There is another experimental result which is worth noting: The behavior $\delta H(E_\perp)$ for electrons above ^{4}He is more complicated than would follow from the theory[66] (Fig. 22). It may be that the discrepancy is due to a slight damping of the ripplons in superfluid ^{4}He, so that the surface does not manage to reach its equilibrium state over the electron relaxation time. For electrons above ^{3}He, which has a high viscosity, the measurements yield $\delta H \propto E_\perp^2$, within experimental error.

9. NONLINEAR EFFECTS

Since the electrons trapped above a helium surface have long relaxation times, and are present in comparatively small numbers, it is possible to observe a variety of nonlinear effects already low levels of power absorbed by the electrons.[7] The primary motivation for studying these effects is that they are of intrinsic interest, but there is also the consideration that such a study could explain the energy-relaxation mechanism and resolve the question of whether the results found in the experiments described in Sections 6–8 refer to equilibrium electrons or to electrons which are superheated with respect to the helium.

Nonlinear effects were reported some time ago.[17,43,55] A study of nonlinear effects in the temperature range in which the electron–ripplon interaction is dominant was begun in Ref. 16 and continued in Ref. 20, in cyclotron-resonance experiments. As reported in Ref. 17, the heating of electrons by the measurement signal, at a power level of $\sim 10^{-8}$ W and at $T \approx 1$ K, i.e., under conditions such that scattering by the gas is predominant, leads to a broadening of the cyclotron-resonance line. A significant decrease in the mobility at $T \approx 1.5$ K was observed in Ref. 55 in fields of the order of 0.1–1 V/cm parallel to the surface; these values correspond to a power dissipation of $\sim 10^{-7}$–10^{-8} erg/(s · electron). The reason for this effect lies in the increase in the electron velocity and thus in the collision frequency resulting from heating. From (30) we easily see that the heating of electrons becomes significant at $\sqrt{2kT_e/m} \approx \sqrt{\pi\hbar\gamma}/2m$, i.e., at $T_e \approx 5$ K. The competing mechanism—the transitions of electrons to excited levels, where the scattering frequency is lower than in the ground state—is less effective.[51]

At low temperatures the picture is different. We see from (35) that the increase $p^2 \propto T_e$ in the presence of a clamping field leads to a decrease in $\nu(p)$ and thus a narrowing of the cyclotron-resonance line[20] (Fig. 23). At the same time, there is a decrease in the shift of the resonance curve, δH, as could be expected on the basis of the mechanism proposed in Refs. 66 and 67: An increase in the quantum number of the Landau level of the electrons participating in the resonance leads both to a decrease in the surface deformation and to a smaller relative change in the orbital dimensions in the transition from n to $n+1$. On the other hand, at this point we cannot explain why δH changes sign, and does not approach zero, as T_e increases. We also note that in all the cases covered in Fig. 23 the change ΔH decreases with increasing P, even at small values of $E_\perp$, at which

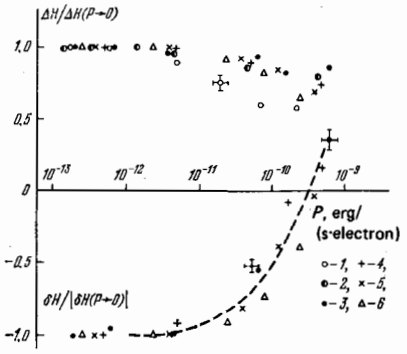

FIG. 23. Dependence of the line width ΔH and the cyclotron-resonance shift δH on the power absorbed at resonance by a single electron.[20] $E_\perp$(V/cm): 1—22; 2—56; 3—460; 4—590; 5—780; 6—1100.

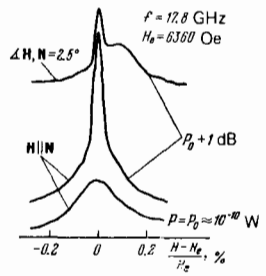

FIG. 24. Amplitude of the 17.8-GHz wave reflected from the resonator as a function of the magnetic field.[16] The surface electron density is $2.2 \cdot 10^7$ cm^{-2}, $E_\perp = 20$ V/cm. The narrower peak, which arises as the power level of the microwave signal is raised, and which does not change position when the magnetic field is inclined at some angle to the normal, is due to a free-electron cyclotron resonance.

the line width should be determined by terms which increase with the temperature, according to (35) (Ref. 69).

At low clamping fields, the electron heating may become so important, at a power level of only $\sim 10^{-10}$ erg/(s·electron), that the electrons go from the $l = 1$ level to the continuum[16] (Fig. 24). Their relaxation time accordingly increases sharply, as can be seen from the appearance of a very narrow resonance line, whose position is independent of the angle between **H** and **N**. For surface electrons, the resonance line shifts toward stronger fields (Fig. 24). Obviously, "free" electrons should be greatly superheated with respect to the bath. Experiments have revealed a change in the width of the cyclotron-resonance line for "free" electrons which is proportional to the square root of the power supplied to the resonator. The minimum width is ~0.15 Oe, which corresponds to $\tau \approx 10^{-6}$ s (cf. the value of ~8 Oe for surface electrons). A calculation from Eq. (29) shows that even at $T_e \approx 10^4$ K and $T = 0.4$ K we should have $\tau \approx 5$ μs and $\Delta H \approx 0.015$ Oe for scattering by vapor atoms. Here T_e cannot exceed 10^4 K, since at a higher energy the electrons would overcome the potential barrier at the interface and escape from the apparatus, but this effect was not observed in the experiments of Ref. 16. It can thus be suggested that the hot electrons are scattered primarily by each other and by vibrations of the helium surface. Further study is required here.

An analogous effect—the heating of electrons and their escape from surface levels—has been observed[9] in a study of surface plasmons [see (22)]. A theory for the hot electrons was derived in Refs. 70–72.

It is difficult to draw quantitative conclusions from the results found in a study of the heating of electrons by the measurement signal, since the temperature of the hot electrons is not known. We would learn more from experiments in which the measurement signal was at a low level, such that there would definitely not be any significant heating, and the deviation from equilibrium in the electron system would be caused by imposing an rf field to cause resonant transitions between levels in the hydrogen-like spectrum in (5). A nonlinear photoresonance of this type was studied in Ref. 20. In those experiments, the cyclotron resonance was monitored at a frequency of 18.5 GHz, and the magnetic field was fixed at the value corresponding to the absorption peak. In addition, a signal whose frequency F lay in the range 130–170 GHz was fed into the resonator. As the clamping field was changed, an increase in the cyclotron absorption at $F = F_{1l}$ was observed (Fig. 25). Amplitude modulation of the signal at the frequency F and the discrimination of the component at the modulation frequency f_{mod} in the measured signal made it possible to measure the relaxation time of the nonequilibrium state, τ_E. Since the response at the frequency f_{mod} was proportional to this quantity under the condition $(2\pi f_{mod}\tau_E)^{-1} \ll 1$, the value $\tau_E = 13 \pm 6$ μs was found from traces like that in Fig. 26.

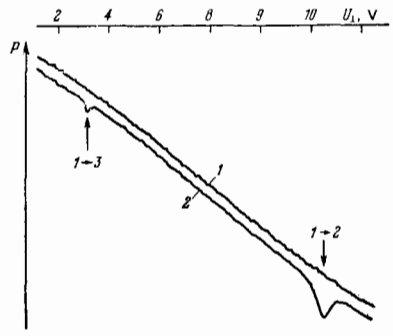

FIG. 25. Dependence on the retarding potential of the 18.5-GHz signal transmitted through the resonator at cyclotron resonance of the electrons above ^{3}He. 1—Without a microwave pump signal; 2—application of microwave power at 108 GHz to the resonator. 1→2 and 1→3—Resonances involving electron transitions from the ground state to the respective excited state.

If $E_\perp$ is fixed such that the amplitude of the variable photoresonance signal is maximized, then its dependence on the magnetic field is easily seen to be described by

$$A(H) \propto \frac{1}{\Delta_1 H(1+\mu_1^2)} - \frac{1}{\Delta_1 H(1+\mu_1^2)}, \quad (\mu_i = e\tau_i(H - H_{res})/mc). \tag{46}$$

In other words, we have the difference between two resonance lines with a width $\Delta_1 H$ for the excited electrons and a width $\Delta_1 H$ for the ground-state electrons. By determining $\Delta_1 H$ in an independent experiment from the width of the cyclotron-resonance line, we can determine $\Delta_1 H$ from traces like that in Fig. 27. The re-

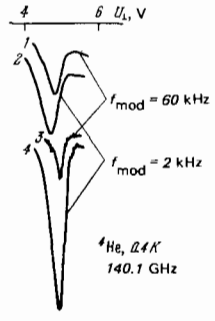

FIG. 26. Dependence on the retarding potential of the constant (1, 2) and varying (3, 4) components of the photoresonance signal for various modulation frequencies.[20] Curve 4 was recorded at a gain one-third that for curve 3.

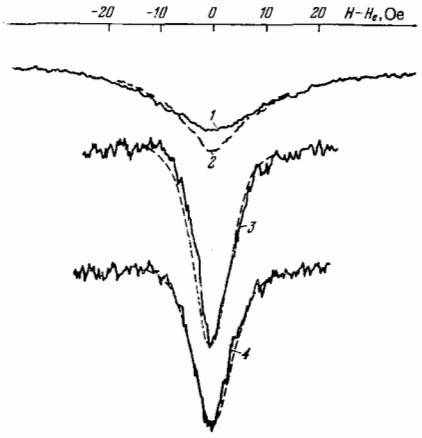

FIG. 27. 1—Magnetic-field dependence of the signal transmitted through the resonator[20]; 2—the same, with a pump signal applied at 135 GHz, causing 1→2 transitions; 3,4—H dependence of the varying component of the photoresonance signal for $F=135$ GHz (the 1→2 transition) and 169.2 GHz (the 1→3 transition); dashed curve-line shape calculated for $\Delta_2 H/\Delta, H=0.5$ and $\Delta_3 H/\Delta, H=0.5$, $E_\perp=12.8$ V/cm. The ^{4}He temperature was 0.4 K.

sulting values of $\Delta_2 H$ are shown in Fig. 21. According to Fig. 27, $\Delta_3 H \approx \Delta_2 H$. For electrons above ^{3}He with $E_\perp \approx 45$ V/cm, the value $\Delta_3 H \approx (0.9 \pm 0.1)\Delta_1 H$ has been found.

In summary, the width of the cyclotron-resonance line for excitation of the 1→2 transition is the same as the width for excitation of the 1→3 transition. On the other hand, since the electrons in the $l=3$ state are much farther from the surface than those in the $l=2$ state (Section 2), we might expect the interaction of the $l=3$ electrons with the ripplons to be much weaker.

The fact that a narrowing of the cyclotron-resonance line is not observed apparently means that there is a relaxation of the electron to a ground state in terms of the z coordinate, to a Landau level $n \approx 2\pi F_{11}/\Omega$, in a short time which is determined by collisions involving a momentum loss. (We recall that for electrons above ^{4}He the value of F_{12} is approximately the same as F_{13} for the experimental conditions of Ref. 20.) This relaxation scheme also corresponds to the result found for electrons above ^{3}He: In scattering by a gas, the calculated width of the cyclotron-resonance line in the $l=3$ state is narrower than that in the $l=1$ state by a factor of 5.6. In this case we should expect the width of the cyclotron-resonance line to be roughly the same as for the resonance in which electrons are heated to a temperature $kT \approx n\hbar\Omega$. Also taking into account the fact that the width of the cyclotron-resonance line decreases by a factor of about two in the excitation of a photoresonance (Fig. 26), we find from Fig. 23 [the $\Delta H(P)$ curve for $E_\perp=22$] that the electrons are heated by $\sim 2\pi\hbar F_{12}/k \approx 6$ K when the power absorption is $\sim 10^{-10}$ erg/(s·electron). According to the theoretical estimate reached in Ref. 68 on the basis of the change $\delta H(P)$, the superheating is an order of magnitude less. Assuming that the superheating is proportional to the power (i.e., that the relaxation time is independent of the temperature), and using the energy balance equation, we find $\tau_E \approx 10^{-5}$ s, in excellent agreement—in view of the crudeness of this estimate—with the value given above for τ_E.

Monarkha and Shikin[68,73] have shown that scattering by ripplons with $q \approx p_H/\hbar \approx 10^5$ cm^{-1}, which have frequencies $\omega \sim 3\cdot 10^7$ s$^{-1} \ll \Omega \approx 10^{11}$ s^{-1}, could not cause transitions between Landau levels. The energy relaxation is thus due to the formation of two ripplons with $\omega_q=\Omega/2$ and with oppositely directed momenta. This mechanism leads to an energy relaxation time which is independent of the clamping field, and this conclusion is consistent with experiment (Fig. 23) if it is assumed that identical heating at different values of $E_\perp$ leads to identical relative changes δH and ΔH.

The numerical estimates in Ref. 73 yield $\tau_E \approx 10^{-6}$ s for two-ripplon processes; in view of the large experimental error and the model dependence of the calculation, we can accept this result as consistent with experiment.

There is yet another series of studies dealing with the energy relaxation of surface electrons; this series is concerned with the electron lifetime in the bound state after the clamping field is removed. It should be noted here that, even in the ideal case of an infinite system and a strictly homogeneous clamping field, it is a far from simple matter to determine the relationships between the measured lifetime τ and the relaxation processes. Upon evaporation of electrons, their temperature should drop significantly, with the possible consequence of a change in the observed values of τ by several orders of magnitude.[74]

Under real experimental conditions, with an apparatus of limited dimensions, significant tangential fields with a magnitude $\sim E_\perp$ arise when $E_\perp$ is turned off, because of the Coulomb interaction of electrons. These fields, which are of the order of volts per centimeter in practice, should cause the electrons to escape to the wall because of their high mobility, 10^5–10^7 cm^2/(V·s), in a characteristic time $\tau \approx 10^{-4}$–10^{-5} s, which would be observable in experiments of this kind. Even if this escape does not occur, there will be an extremely high probability for heating of the electrons by the tangential field.[75] These parasitic effects depend on many factors, in particular, the voltage rise time when $E_\perp$ is turned off. We do not know of a single paper in which the experimental procedure was described in such detail that the particular processes responsible for the results could be identified. Since the values which have been measured for τ differ by one or two orders of magnitude, even in experiments by the same workers (see Refs. 75 and 76, for example), it seems premature to discuss the conclusions which could be drawn from such experiments.

10. CONCLUSION

As this review has shown, much has been accomplished in research on the two-dimensional system of electrons trapped above liquid and solid cryogenic dielectrics over the past decade since the discovery of this effect. The liquid-helium experiments furnish a good basis for further development of the theory and for

extending the research to new systems. This work has already begun, and we can expect some interesting new effects in the future.

One problem to which we would like to draw attention is the behavior of the electron spin. On the basis of general considerations we would expect that the spin relaxation times in this case would be extremely long, and the electron magnetization would be retained for a long time. These arguments can be based on experiments on the paramagnetic resonance of negative ions in liquid helium,[77] where values ~1 and >5 μs were found for the transverse spin relaxation times for ^{3}He and ^{4}He. Since the distance from the trapped electrons to the atoms is an order of magnitude greater than the ion radius, these times should increase greatly. However, this question has not yet been taken up, and we lack even crude estimates of the relaxation times of the spin system.

Another effect which may be related to surface electrons was pointed out by Khaĭkin.[23] Radio-astronomy observations of nebulae have revealed emission of appreciable intensity at a frequency near that which would be expected for transitions in the spectrum of electrons trapped above hydrogen. Since the relative abundance of hydrogen in the universe is extremely high, this coincidence deserves study.

Further work on nonlinear effects seems promising. In particular, upon photoexcitation of electrons to the continuum we could expect a narrowing of the cyclotron-resonance line to $\Delta H/H \lesssim 10^{-7}$, which might be exploited to refine the values of the universal constants.

We make no claim that this list of possible directions for future research on trapped electrons is anything like complete. We do not rule out the possibility that absolutely unexpected properties may be found for these electrons. We strongly hope that research on this beautiful natural phenomenon will continue and that we will continue to learn from it.

[1]M. W. Cole and M. H. Cohen, Phys. Rev. Lett. 23, 1238 (1969).
[2]V. B. Shikin, Zh. Eksp. Teor. Fiz. 58, 1748 (1970) [Sov. Phys. JETP 31, 936 (1970)].
[3]J. E. Berthold, H. N. Hanson, H. J. Maris, and G. M. Seidel, Phys. Rev. B14, 1902 (1976).
[4]L. D. Landau and E. M. Lifshitz, Élektrodinamika sploshnykh sred, Fizmatgiz, M., 1959, p. 60 (Electrodynamics of Continuous Media, Addison–Wesley, Reading, Mass., 1960).
[5]L. D. Landau and E. M. Lifshitz, Mekhanika, Nauka, M., 1965, p. 35 (Mechanics, Addison–Wesley, Reading, Mass., 1960).
[6]M. W. Cole, Rev. Mod. Phys. 46, 451 (1974).
[7]V. B. Shikin and Yu. P. Monarkha, Fiz. Nizk. Temp. 1, 957 (1975) [Sov. J. Low Temp. Phys. 1, 459 (1975)].
[8]R. S. Crandall, Surf. Sci. 58, 266 (1976).
[9]C. C. Grimes, Surf. Sci. 73, 379 (1978).
[10]C. C. Grimes, T. R. Brown, M. L. Burns, and C. L. Zipfel, Phys. Rev. B13, 140 (1976).
[11]M. A. Woolf and G. W. Rayfield, Phys. Rev. Lett. 15, 235 (1965).
[12]H. A. Kierstead, J. Low Temp. Phys. 24, 497 (1976).
[13]A. P. Volodin and V. S. Édel'man, Pis'ma Zh. Eksp. Teor. Fiz. 30, 668 (1979) [JETP Lett. 30, 633 (1979)].
[14]M. W. Cole, Phys. Rev. B2, 4239 (1970).
[15]V. S. Édel'man, Pis'ma Zh. Eksp. Teor. Fiz. 24, 510 (1976) [JETP Lett. 24, 468 (1976)].
[16]V. S. Édel'man, Pis'ma Zh. Eksp. Teor. Fiz. 25, 422 (1977) [JETP Lett. 25, 394 (1977)].
[17]T. R. Brown and C. C. Grimes, Phys. Rev. Lett. 29, 1233 (1972).
[18]W. T. Sommer, Phys. Rev. Lett. 12, 271 (1964).
[19]V. S. Édel'man, Pis'ma Zh. Eksp. Teor. Fiz. 26, 647 (1977) [JETP Lett. 26, 493 (1977)].
[20]V. S. Édel'man, Zh. Eksp. Teor. Fiz. 77, 673 (1979) [Sov. Phys. JETP 50, 338 (1979)].
[21]A. M. Troyanovskiĭ, A. P. Volodin, and M. S. Khaĭkin, Pis'ma Zh. Eksp. Teor. Fiz. 29, 65 (1979) [JETP Lett. 29, 59 (1979)].
[22]A. M. Troyanovskiĭ, A. P. Volodin, and M. S. Khaĭkin, Pis'ma Zh. Eksp. Teor. Fiz. 29, 421 (1979) [JETP Lett. 29, 382 (1979)].
[23]M. S. Khaĭkin, Pis'ma Zh. Eksp. Teor. Fiz. 27, 706 (1978) [JETP Lett. 27, 668 (1978)].
[24]A. S. Rybalko and Yu. Z. Kovdrya, Fiz. Nizk. Temp. 1, 1037 (1975) [Sov. J. Low Temp. Phys. 1, 498 (1975)].
[25]A. P. Volodin, M. S. Khaĭkin, and V. S. Édel'man, Pis'ma Zh. Eksp. Teor. Fiz. 23, 524 (1976) [JETP Lett. 23, 478 (1976)].
[26]S. A. Govorkov and V. A. Tulin, Fiz. Nizk. Temp. 3, 1093 (1977) [Sov. J. Low Temp. Phys. 3, 532 (1977)].
[27]L. D. Landau and E. M. Lifshitz, Kvantovaya mekhanika, Fizmatgiz, M., 1963, p. 209 (Quantum Mechanics: Non-relativistic Theory, Addison–Wesley, Reading, Mass., 1971).
[28]V. B. Shikin, Author's Abstract, Doctoral Dissertation, Institute of Physical Problems, Academy of Sciences of the USSR, Moscow, 1973.
[29]L. P. Gor'kov and D. M. Chernikova, Pis'ma Zh. Eksp. Teor. Fiz. 18, 119 (1973) [JETP Lett. 18, 68 (1973)]; Dokl. Akad. Nauk SSSR 228, 829 (1976) [Sov. Phys. Dokl. 21, 328 (1976)].
[30]D. M. Chernikova, Fiz. Nizk. Temp. 2, 1374 (1976) [Sov. J. Low Temp. Phys. 2, 669 (1976)].
[31]C. W. F. Everitt, K. R. Atkins, and A. Denenstein, Phys. Rev. A136, 1494 (1964).
[32]A. P. Volodin, M. S. Khaĭkin, and V. S. Édel'man, Pis'ma Zh. Eksp. Teor. Fiz. 26, 707 (1977) [JETP Lett. 26, 543 (1977)].
[33]V. B. Shikin, Pis'ma Zh. Eksp. Teor. Fiz. 27, 44 (1978) [JETP Lett. 27, 39 (1978)].
[34]M. Wanner and P. Leiderer, Phys. Rev. Lett. 42, 315 (1979).
[35]P. Leiderer and M. Wanner, Phys. Lett. A73, 189 (1979).
[36]R. S. Crandall, Phys. Rev. A8, 2136 (1973).
[37]P. M. Platzman and H. Fukuyama, Phys. Rev. B10, 3150 (1974).
[38]T. Nagai and A. Onuki, J. Phys. C 11, L681 (1978).
[39]R. W. Hockney and T. R. Brown, J. Phys. C 8, 1813 (1975).
[40]W. Huang, J. Rudnick, and A. J. Dahm, J. Low Temp. Phys. 28, 21 (1977).
[41]Yu. P. Monarkha and V. B. Shikin, Zh. Eksp. Teor. Fiz. 68, 1423 (1975) [Sov. Phys. JETP 41, 710].
[42]H. Fukuyama, Sol. State Comm. 17, 1323 (1975).
[43]C. C. Grimes and G. Adams, Phys. Rev. Lett. 36, 145 (1976).
[44]C. C. Grimes and G. Adams, Surf. Sci. 58, 292 (1976).
[45]C. L. Zipfel, T. R. Brown, and C. C. Grimes, Phys. Rev. Lett. 37, 1760 (1976).
[46]V. B. Shikin, Pis'ma Zh. Eksp. Teor. Fiz. 22, 328 (1975) [JETP Lett. 22, 154 (1975)].
[47]D. S. Fisher, B. I. Halperin, and P. M. Platzman, Phys. Rev. Lett. 42, 798 (1979).
[48]C. C. Grimes and G. Adams, Phys. Rev. Lett. 42, 795 (1979); Yamada Conference II on Electronic Properties of Two-Dimensional Systems: Third International Conference, Japan, 1979 (proceedings to be published in Surface Science).

[49]A. S. Rybalko, B. N. Esel'son, and Yu. Z. Kovdrya, Fiz. Nizk. Temp. 5, 947 (1979) [Sov. J. Low Temp. Fiz. 5, 450 (1979)].
[50]Yu. P. Monarkha, Fiz. Nizk. Temp. 5, 950 (1979) [Sov. J. Low Temp. Phys. 5, 451 (1979)].
[51]R. S. Crandall, Phys. Rev. A6, 790 (1972); B12, 119 (1975).
[52]B. Bederson and L. J. Kieffer, Rev. Mod. Phys. 43, 601 (1971).
[53]W. T. Sommer and D. J. Tanner, Phys. Rev. Lett. 27, 1345 (1971).
[54]A. S. Rybalko, Yu. Z. Kovdrya, and B. N. Esel'son, Pis'ma Zh. Eksp. Teor. Fiz. 22, 569 (1975) [JETP Lett. 22, 280 (1975)].
[55]F. Bridges and J. F. McGill, Phys. Rev. B15, 1324 (1977).
[56]T. P. Eggarter and M. H. Cohen, Phys. Rev. Lett. 27, 129 (1971).
[57]T. Ando, J. Phys. Soc. Jpn. 44, 765 (1978).
[58]K. R. Atkins, Canad. J. Phys. 31, 1165 (1953).
[59]V. B. Shikin and Yu. P. Monarkha, J. Low Temp. Phys. 16, 193 (1974).
[60]Yu. P. Monarkha, Fiz. Nizk. Temp. 2, 1232 (1976) [Sov. J. Low Temp. Phys. 2, 600 (1976)].
[61]P. M. Platzman and G. Beni, Phys. Rev. Lett. 36, 626 (1976).
[62]B. N. Esel'son, A. S. Rybalko, Yu. Z. Kovdrya, A. A. Golub, and S. S. Sokolov, in: Materialy 20-go Vsesoyuznogo soveshchaniya po fizike nizkikh temperatur (Proceedings of the Twentieth All-Union Conference on Low-Temperature Physics), Chernogolovka, 1978, Moscow, Part II, p. 280.
[63]M. I. Dykman and L. S. Khazan, Zh. Eksp. Teor. Fiz. 77, 1488 (1979) [Sov. Phys. JETP 50, 747 (1979)].
[64]V. B. Shikin, Zh. Eksp. Teor. Fiz. 60, 713 (1971) [Sov. Phys. JETP 33, 387 (1971)].
[65]V. B. Shikin and Yu. P. Monarkha, Zh. Eksp. Teor. Fiz. 65, 751 (1973) [Sov. Phys. JETP 38, 373 (1974)].
[66]A. Cheng and P. M. Platzman, Sol. State Comm. 25, 813 (1978).
[67]V. B. Shikin, Zh. Eksp. Teor. Fiz. 77, 717 (1979) [Sov. Phys. JETP 50, 360 (1979)].
[68]Yu. P. Monarkha and V. B. Shikin, Cited on p. 555 in Ref. 48.
[69]Yu. P. Monarkha and S. S. Sokolov, Fiz. Nizk. Temp. 4, 685 (1978) [Sov. J. Low Temp. Phys. 4, 327 (1978)].
[70]V. B. Shikin, Pis'ma Zh. Eksp. Teor. Fiz. 25, 425 (1977) [JETP Lett. 25, 397 (1977)].
[71]T. Aoki and M. Saitoh, J. Phys. Soc. Jpn. 46, 423 (1979).
[72]M. Saitoh and T. Aoki, Cited in Ref. 48.
[73]Yu. P. Monarkha, Fiz. Nizk. Temp. 4, 1093 (1978) [Sov. J. Low Temp. Phys. 4, 515 (1978)].
[74]R. S. Crandall, Phys. Rev. A9, 1297 (1974).
[75]Y. Iye, K. Kŏno, K. Kajita, and W. Sasaki, J. Low Temp. Phys. 34, 539 (1979).
[76]K. Kŏno, Y. Iye, K. Kajita, S. Kobayashi, and W. Sasaki, Cited in Ref. 48.
[77]J. F. Reichert, N. Jarošik, R. Herrick, and J. Andersen, Phys. Rev. Lett. 42, 1359 (1979).
[78]V. S. Édel'man, Usp. Fiz. Nauk 126, 694 (1978) [Sov. Phys. Usp. 21, 1008 (1978)].

Translated by Dave Parsons